Mechanical Properties of Bacterially Synthesized Nanocellulose Hydrogels

Mareike Frensemeier,[1,3] *Christof Koplin,*[1] *Raimund Jaeger,**[1] *Friederike Kramer,*[2] *Dieter Klemm**[2]

Summary: The mechanical characteristics of bacterially synthesized nano-cellulose (BNC) were studied with uniaxial compression and tensile tests. Compressive loads result in a release of water and the deformation of the water-saturated network corresponds approximately to the volume of released water. The BNC hydrogel exhibits a mainly viscous response under compression. The strain response under tensile loads has an elastic and a viscous component. This can be described with a Maxwell model, where the viscosity is strain rate-dependent. When the aqueous phase of the BNC hydrogel is stabilized with an additional alginate hydrogel matrix, the system exhibits an elastic response under compressive loads. The analysis of the 'alginated' BNC network with the Maxwell model shows that the alginate matrix increases the viscosity of the composite system. The results of the mechanical tests show that the water absorbed in the BNC hydrogel strongly influences its mechanical behavior.

Keywords: bacterially synthesized nanocellulose; elastic response; fibers; hydrogels; mechanical properties; viscous response

Introduction

Polysaccharide cellulose is an almost inexhaustible polymeric raw material with fascinating structure and properties. Formed by the repeated connection of D-glucose building blocks, the highly functionalized, linear stiff-chain homopolymer is characterized by its hydrophilicity, chirality, biodegradability, broad chemical modifying capacity, and its formation of versatile semicrystalline fiber morphologies.[1]

Not only plants, but also bacteria are able to produce cellulose. One of the most efficient cellulose producers is *Gluconacetobacter xylinus*. This bacterium synthesizes cellulose fleeces in static culture at the air - liquid interface from a culture medium which contains D-glucose.[2] The bacterially synthesized nanocellulose (BNC) is characterized by a supramolecular structure quite different from plant cellulose. It is composed of a network of cellulose nanofibers which are able to hold more than 99 wt% of water forming a hydrogel.[3] The BNC nanofibers are characterized by high crystallinity of 70-80%[2] and a high degree of polymerization with repeating units of about 2,000-10,000.[4,5] Furthermore, the BNC is free of accompanying substances – like lignin, pectin, and hemicelluloses which are found in plant celluloses as well as foreign functionalities like –CO or –COOH and therefore is highly pure. Even in a wet state, BNC is mechanically stable. The fiber aggregates have a Young's modulus of up to 134 GPa and the tensile strength of single fibers is 2 GPa, which is in the range of steel or aramid fibers (Kevlar).[6–8]

Due to its biocompatibility[1,9], BNC is a promising biomedical material useful for

[1] Fraunhofer Institute for Mechanics of Materials, Biomedical Materials and Implants - Group, Wöhlerstr. 11, 79108 Freiburg, Germany
Fax: (+49) 761 5142 403;
E-mail: raimund.jaeger@iwm.fraunhofer.de
[2] Polymet Jena – Transfer group at Friedrich-Schiller-Universität Jena, Wildenbruchstr. 15, 07745 Jena, Germany
Fax: (+49) 3641 548 288;
E-mail: dieter.klemm@polymet-jena.de
[3] Current address: Saarland University, Department Materials Science, Institute of Functional Materials, Campus D33, 66123 Saarbrücken, Germany

external application (it is an already established material for wound dressings). In addition, it has a high potential for the development of bioactive implants. Due to the fact that it is composed of a fibrous network and an aqueous phase, it could potentially be used as a replacement material for cartilage or an in vivo-scaffold for tissue repair. Cartilage has a bi-phasic structure which leads to its unique mechanical and tribological properties[10]: it consists of a fibrous, poro-elastic structure, which holds a liquid phase. Under pressure, the liquid phase is partially released and acts as a lubricant for joints. Since cartilage is a load-bearing tissue, investigating its mechanical properties is a first step in assessing the applicability of BNC as a biomedical material and optimizing its performance.[11] In addition to investigating the mechanical properties of »pure« BNC, the aqueous phase of BNC was modified with an additional alginate hydrogel matrix. Alginates were chosen since they support chondrocytes[12] and chondrogenesis[13] and are biocompatible in delivering cells in human trials.[14]

There are only a few papers which report on systematic and extensive measurements of the mechanical properties of never-dried and dewatered BNC as well as of BNC composites. Astley et al.[15] have described the tensile deformation of BNC and its composites with xyloglucan and pectin and shown by uniaxial deformation experiments how the cellulose microfibrils reorient during deformation. Systematic studies of preparation and mechanical properties of double network hydrogels formed from BNC and gelatin, sodium alginate, gellan gum, and t-carrageenan were reported by the research group of Jian Ping Gong.[16,17] These composites are described as potential materials for producing artificial cartilage. A moisture-induced softening of BNC/glucuronoxylan nanocomposites could be demonstrated by dynamical mechanical measurements.[18] Millon and Wan[19] have characterized the stress-strain properties of polyvinyl alcohol-BNC composites with respect to its application as biomaterial.

Materials and Methods

Specimens

In order to prepare the BNC-sheets, the bacteria strain *Gluconacetobacter xylinum* (DSMZ 14666 – DSM: Deutsche Sammlung für Mikroorganismen und Zellkulturen Braunschweig) was used. The bacteria were cultivated in polypropylene dishes (10 x 20 cm). 500 ml of Hestrin-Schramm-Medium[20] sterilized in a pressure cooker at 121 °C for 20 minutes was inoculated with 25 ml of a 7 d old liquid pre-culture. After static culture at 28 °C for 7 d the cellulose fleeces – which had a thickness of about 5 - 10 mm – were taken from the culture medium, washed with distilled water, treated with boiling 0.1 N aqueous sodium hydroxide for 60 min, and washed with distilled water to a neutral reaction of the rinsing agent.

All specimens were prepared from BNC sheets which were previously never dried, i.e. the material was continuously in contact with an aqueous medium. Specimens for mechanical testing were cut from BNC-sheets with a circular saw. Special care was taken to minimize a deformation (and the resulting release of water) of the specimens prior to the mechanical tests. For the compression tests, cube-shaped specimens were prepared (base area: 10×10 mm, height 10 - 15 mm, depending on the thickness of the BNC-sheet). For the tensile tests, tapered tensile specimens (dimension: $105 \times 7 \times 5$ mm) were cut.

In order to infiltrate the BNC network with an alginate hydrogel, the specimens were submerged in sodium alginate solution (5 mg / ml) at 32 °C for 60 h. The alginate was cross-linked by placing the specimens in an aqueous $CaCl_2$ solution (5 mg / ml) for 15 min.

Mechanical Testing

Compression tests were carried out with an electro-magnetic mechanical tester (Shaker 4808, Brüel & Kjær, Nærum, Denmark) which was controlled with Labview software. The specimens were compressed with a cylindrical plunger (diameter 23 mm).

The testing arrangement was contained in a transparent Plexiglas outer cylinder (diameter 26 mm). The amount of released water could be determined by measuring the height of the water column in the Plexiglas cylinder. Sample dimensions and the height of the water columns were documented with a digital camera (Ricoh Caplio R4). Images were taken every 5 or 10 seconds.

A servo-hydraulic mechanical tester (MTS 858 MiniBionix II, MTS Systems Corporation, Eden Prairie, USA) was used for the tensile tests. The tensile specimens were mounted in stainless steel sample grips.

All experiments were carried out in displacement control. In order to investigate the mechanical response of the specimens, a linear displacement ramp with resting periods was applied. The force which resulted from the sample deformation was recorded. The compression tests were carried out with a strain rate of 0.2 mm/s (pure BNC) or 0.04 mm/s (alginated BNC), the tensile tests with a strain rate of 0.2 mm/s and 0.02 mm/s.

Mechanical Model

An initial analysis of the mechanical behavior of the BNC with a Burgers model[21] (which includes an elastic, a visco-elastic and a viscous mechanical response) showed that a simple Maxwell model with an additional swelling component and strain-dependent moduli and volume was sufficient to describe the mechanical behavior of the BNC (ε: strain, E: Young's modulus, η: viscosity, σ: stress, v: relative Volume):

$$\varepsilon = \left[{}^{1}/_{E} + {}^{dt}/_{\eta}\right] \cdot \sigma + {}^{v}/_{3}, \quad E, \eta, v = f(\varepsilon). \tag{1}$$

The experimental data for the strain were fitted with the model using a simple backward Euler procedure:

$$\varepsilon(t + \Delta t) = \varepsilon(t) + \Delta t \cdot {}^{d\varepsilon(t)}/_{dt}.$$

We assumed that changes in the moduli can be neglected:

$$E \cdot {}^{d\varepsilon}/_{dt} >> \varepsilon \cdot {}^{dE}/_{dt}.$$

During the tensile experiments a 'necking' of the specimens occurs. The necking leads to an inhomogeneous spatial distribution of stresses, strains, and - as a result - to a locally increased water loss and volume reduction. The development of the specimen cross-section during the tensile tests was analyzed by image processing. Based on the results of the compression tests (see the following section), we assumed that the volume change of the specimen during the tensile tests is entirely due to the loss of released water v (i.e. apart from the water release, the system is incompressible). In addition, we assumed that the release of water increases linearly with the strain. As a result, the following relation holds:

$$\varepsilon_{axial} = \varepsilon_{transversal} = -v. \tag{2}$$

Results

Pure BNC: Compression Tests

Applying a compressive force on the BNC cubes results in a release of the water which is contained in the fiber network. The development of the water release and the deformation of the cube are shown in Figure 1. The compression of the cube does not result in a significant change of the lateral dimension x_i of the specimen. The volume of the cube was determined in three different ways: it was determined by analyzing the images of the deformed cube which were taken during the experiment, assuming a square base area of the specimen during the experiment: $V(z_i) = z_i \cdot x_i^2$ (denoted by the symbol + in Figure 1, z_i: specimen height, x_i: lateral dimension). In addition, the volume was determined assuming that the reduction of the cube's volume equals the volume $V_{released}(z_i)$ of water released at a specimen height z_i: $V(z_i) = V(z_0) - V_{released}(z_i)$. The volume of the released water was either determined

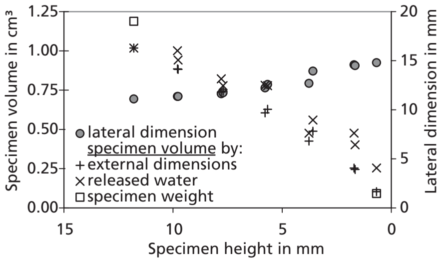

Figure 1.
Sample deformation and specimen volume during a compression test of a BNC cube (strain rate 0.2 mm/s). The specimen volume was determined by the outer dimensions of the cube ('external dimensions': +) and by the amount of released water which was determined by the fluid level in the Plexiglas cylinder ('released water': ×) and by the weight of the sample ('specimen weight':□).

by the height of the water column in the Plexiglas cylinder (denoted by symbol × in Figure 1), or by weighing the specimen before and after the experiment and calculating the amount of water: $V_{released}(z_f) = \rho_{water}^{-1} \cdot (m(z_0) - m(z_f))$ (denoted by symbol □ in Figure 1, ρ_{water}: density water, m(z): mass of the specimen). The results of the different ways to determine the volume of the specimen during the compression test agree very well, i.e. the assumption that the reduction of the cube's volume equals the amount of water released is correct: the deformation of the cube is largely caused by the transport of the water which was contained in the network.

True stress and true strain during a compression test with rest periods are displayed in Figure 2. The true strain is defined as $\varepsilon = -\ln(z(t)/z(0))$, i.e. a true strain of $\varepsilon = 2$ corresponds to a compression of the cube to 13.5% of its original height. No significant elastic response of the specimens is observed during the resting periods for true strains $\varepsilon < 1$. The force response of the BNC for low strains is almost purely viscous: forces occur only when the plunger is moved downwards. For true strains $\varepsilon > 1$, a significant increase of the force which is necessary to compress the specimen is observed. In addition, the specimen exhibits a small elastic response during the resting periods: a finite force is required to maintain the compression of the specimen during the resting periods.

The specimen does not recover its original shape when the plunger is moved back; it essentially remains in its compressed state.

Experimental data were used to determine the strain dependent model parameters of the Maxwell model (see Equation 1) employing a least square fit. The strain-dependent dynamic viscosity shows a significant increase for true strains $\varepsilon > 1$. In addition, it is necessary to use the elastic component of the model function in order to describe the true strain as a function of the stress adequately (see Figure 2).

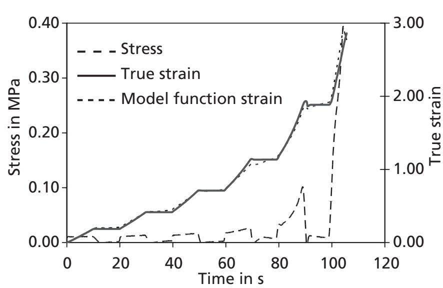

Figure 2.
True stress, true strain and model function for the strain during a compression test of a BNC cube, strain rate 0.2 mm/sec.

Pure BNC: Tensile Tests

Under tensile loading, the BNC specimens exhibit a more complex force response (see Figure 3). The stresses do not vanish during

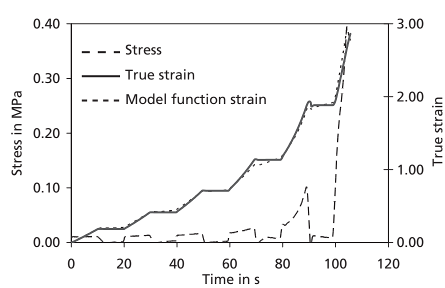

Figure 3.
Stress, strain and model function for the strain of a tensile test of a BNC specimen, strain rate 0.2 mm/s. The sample is tested until its ultimate tensile strength (approx. 9 MPa) is reached.

the resting periods of the sample grips and a stress relaxation is observed if the strain is kept at a constant value. As for the compression tests, the compliance of the BNC specimens is reduced at higher strains. The analysis of the experimental data with the mechanical model (Equation 1) yields strain dependent values for the elastic modulus E(ε) and the dynamic viscosity η(ε) (see Figure 5). Both parameters increase significantly at higher strains.

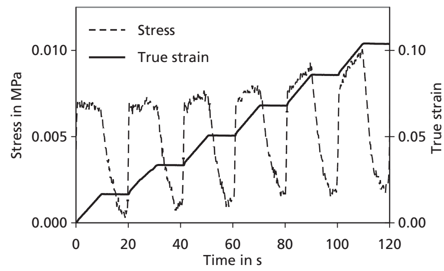

Figure 4.
Stress and true strain of a compression test of an alginated BNC cube, strain rate: 0.04 mm/s. The specimen exhibits an elastic response during the resting periods: a finite stress remains during the resting periods of the plunger.

Mechanical Tests on Alginated BNC

The infiltration of the BNC network with an alginate gel changes the mechanical properties of the specimens. One effect of the infiltration which is immediately noticeable when handling the specimens is their increased dimensional stability. Furthermore, it was necessary to reduce the strain rate to 0.04 mm/s in order to achieve a stable experimental procedure and to be able to analyze the stress response of a system with slowed-down transport processes. The result of a compression test is displayed in Figure 4. In contrast to pure BNC, the alginated BNC exhibits an elastic response during the resting periods of the plunger even at low strains: the stress is only partially relaxed.

The shape of the stress-strain curve of the tensile tests on alginated BNC specimens resembles the curves of the pure BNC samples. An analysis of the tensile tests of the alginated BNC with the mechanical model shows the differences between the two types of specimens. Pure and alginated BNC exhibit a similar development of the strain-dependent modulus (see Figure 5, diagram on the left). The algination results, however, in a significant increase of the dynamic viscosity of the material (Figure 5, diagram on the right).

Discussion

The mechanical tests on the BNC show that the transport of water which is contained in the BNC networks plays a dominant role for its mechanical properties. In compression tests, the compression of the specimens equals essentially the amount of released water, i.e. in order to achieve a plastic deformation of the sample, the corresponding amount of water has to be released from the network. The system exhibits an essentially viscous mechanical behavior at

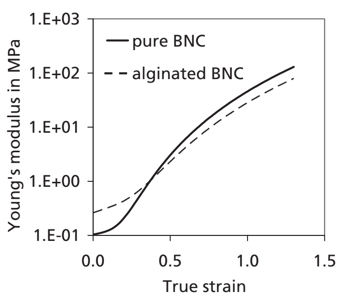

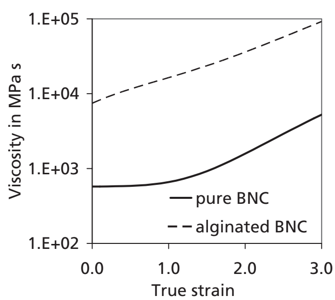

Figure 5.
Development of the strain-dependent parameters of the Maxwell model during a tensile test of pure and alginated BNC.

low compressive strains. The fiber network does not contribute directly to the force response at low strains, since the fibers can re-arrange under compression and relax the applied stress. At higher compressive strains, the force response of the BNC starts to show an elastic component which is most likely due to the resilience of the highly compressed fiber network.

Since the fibers are clamped by the sample grips in tensile tests, the sample grips exert a tensile force on the fiber network during the tests. Fibers which are clamped in both grips or which are strongly entangled in the network will not be able to reduce completely the applied tensile stresses by rearranging their position. As a result, the system exhibits an elastic component of the force response in addition to the viscous response.

The increasing values of the parameters E and η of the Maxwell model for increasing strains reflect the changes in the fiber network. High strains result in a close packing of the fibers which hinders the transport of water. Tensile loads result in an increased orientation of the fibers in the force direction such that the effective elastic modulus of the network increases.

Since the transport of water in the network strongly influences the mechanical properties of pure BNC at low strains, the infiltration of the fiber network with an alginate hydrogel changes the mechanical properties of the system. The alginate matrix results in an improved dimensional stability of the alginated BNC. The alginate hydrogel partially hinders the release of water from the network and results in an elastic force response at low compressive strains. The elastic response of the alginated BNC network under tensile loads is dominated by the elastic response of the fiber network: pure and alginated BNC exhibit a similar development of the parameter $E(\varepsilon)$ of the Maxwell model. The alginate matrix, however, strongly influences the viscosity $\eta(\varepsilon)$ of the Maxwell model which is related to the fluid transport in the network.

An insight into the mechanical behavior of BNC is a pre-requisite for its future application as a biomedical material. The currents study shows that the mechanical performance of the BNC network can be influenced by an additional alginate hydrogel matrix. The next steps in assessing the potential of alginate-modified BNC networks as biomedical material in cartilage repair include tests which simulate appropriate physiological load situations, e.g. tribological tests. Initial studies on biomechanical properties of double-network hydrogels show promising results.[22]

[1] D. Klemm, B. Heublein, H.-P. Fink, A. Bohn, *Angew. Chem. Int. Ed.* **2005**, *44*, 3358.
[2] D. Klemm, D. Schumann, F. Kramer, N. Heßler, M. Hornung, H.-P. Schmauder, S. Marsch, *Adv. Polym. Sci.* **2006**, *205*, 49.
[3] K. Gelin, A. Bodin, P. Gatenholm, A. Mihranyan, K. Edwards, M. Strømme, *Polymer* **2007**, *48*, 7623.
[4] S. Salmon, S. M. Hudson, *J. Macromol. Sci. Rev. Macromol. Chem. Phys.* **1997**, *C37*, 199.
[5] S. Yamanaka, K. Watanabe, in "*Cellulosic Polymer Blends and Composites*", R. D. Gilbert, Eds. Hauser Verlag, München 1994.
[6] H. Yano, J. Sugiyama, A. N. Nakagaito, M. Nogi, T. Matsuura, M. Hikita, K. Handa, *Adv. Mater.* **2005**, *17*, 153.
[7] H. Yano, S. Nakahara, *J. Mater. Sci.* **2004**, *39*, 1635.
[8] G. Guhados, W. Wan, J. L. Hutter, *Langmuir* **2005**, *21*, 6642.
[9] D. Klemm, D. Schumann, U. Udhardt, S. Marsch, *Prog. Polym. Sci.* **2001**, *26*, 1561.
[10] V. C. Mow, M. H. Holmes, W. M. Lai, *J. Biomechanics* **1984**, *17*, 377.
[11] M. Frensemeier, "*Potentialanalyse zur bionischen Optimierung von Hydrogelen am Beispiel fibrillärer Bakterien-Nanozellulose*", Bachelor thesis, University of Applied Sciences Bremen, **2008**.
[12] H. J. Hauselmann, R. J. Fernandes, S. S. Mok, T. M. Schmid, J. A. Block, M. B. Aydelotte, *J. Cell. Sci.* **1994**, *107*, 17.
[13] S. C. Chang, G. Tobias, A. K. Roy, C. A. Vacanti, L. J. Bonassar, *Plast. Reconstr. Surg.* **2003**, *112*, 793.
[14] C. A. Vacanti, L. J. Bonassar, M. P. Vacanti, J. Shufflebarger, *N. Engl. J. Med.* **2001**, *344*, 1511.
[15] O. M. Astley, E. Chanliaud, A. M. Donald, M. J. Gindley, *Int. J. Biol. Macromol.* **2003**, *32*, 28.
[16] A. Nakayama, A. Kakugo, J. P. Gong, Y. Osada, M. Takai, T. Erata, S. Kawano, *Adv. Funct. Mater.* **2004**, *14*, 1124.
[17] C. Azuma, K. Yasuda, Y. Tanabe, H. Taniguro, F. Kanaya, A. Nakayama, Y. M. Chen, J. P. Gong, Y. Osada, *J. Biomed. Mater. Res., Part A* **2007**, *81A*, 373.

[18] S. Dammstroem, L. Salmen, P. Gatenholm, *Polymer* **2005**, *46*, 10364.
[19] L. E. Millon, W. K. Wan, *J. Biomed. Mater. Res., Part B* **2006**, *79*, 245.
[20] S. Hestrin, M. Schramm, *Biochem.* **1954**, *58*, 345.
[21] J. M. Burgers, *Verh. K. Akad. Wet. Amsterdam* **1935**, *15*, 5.
[22] K. Yasuda, J. P. Gong, Y. Katsuyama, A. Nakayama, Y. Tanabe, E. Kondo, M. Ueno, Y. Osada, *Biomaterials*, **2005**, *26*, 4468.

